

## Structure-Based Design and Synthesis of Non-Nucleoside, Potent, and Orally Bioavailable Adenosine Deaminase Inhibitors

Tadashi Terasaka,<sup>\*,†</sup> Hiroyuki Okumura,<sup>†</sup> Kiyoshi Tsuji,<sup>†</sup> Takeshi Kato,<sup>†</sup> Isao Nakanishi,<sup>‡,‡</sup> Takayoshi Kinoshita,<sup>‡</sup> Yasuko Kato,<sup>§</sup> Masako Kuno,<sup>§</sup> Nobuo Seki,<sup>§</sup> Yoshinori Naoe,<sup>§</sup> Takeshi Inoue,<sup>§</sup> Kohichiro Tanaka,<sup>||</sup> and Katsuya Nakamura<sup>†</sup>

Medicinal Chemistry Research Laboratories, Basic Research Laboratories, Medicinal Biology Research Laboratories, and Biopharmaceutical and Pharmacokinetic Research Laboratories, Fujisawa Pharmaceutical Co., Ltd., 2-1-6, Kashima, Yodogawa-ku, Osaka 532-8514, Japan

Received January 15, 2004

**Abstract:** We disclose optimization efforts based on the novel non-nucleoside adenosine deaminase (ADA) inhibitor, **4** ( $K_i = 680$  nM). Structure-based drug design utilizing the crystal structure of the **4**/ADA complex led to discovery of **5** ( $K_i = 11$  nM, BA = 30% in rats). Furthermore, from metabolic considerations, we discovered two inhibitors with improved oral bioavailability [**6** ( $K_i = 13$  nM, BA = 44%) and **7** ( $K_i = 9.8$  nM, BA = 42%)]. **6** demonstrated in vivo efficacy in models of inflammation and lymphoma.

Adenosine deaminase (ADA) (EC. 3.5.4.4) is a key enzyme in purine metabolism and catalyzes the irreversible deamination of adenosine and 2'-deoxyadenosine to inosine and 2'-deoxyinosine, respectively.<sup>1</sup> ADA is ubiquitous in almost all human tissues and is assumed to play a crucial role in the development of the immune system because genetic ADA deficiency results in severe combined immunodeficiency disease by impairment of the differentiation and maturation of lymphoid cells.<sup>2</sup> ADA abnormalities have also been reported in a variety of other diseases,<sup>3</sup> such as rheumatoid arthritis<sup>4</sup> and leukemia.<sup>5</sup> In recent years, adenosine has come to be considered as an important factor in the attenuation of inflammation,<sup>6,7</sup> since it has been reported that the concentration of adenosine is increased in inflammatory lesions.<sup>8</sup> Furthermore, it is also believed that ecto-ADA has an extra enzymatic function via binding with CD26 on the surface of activated lymphocytes<sup>9</sup> and could perpetuate chronic inflammation by metabolizing adenosine released at inflamed sites that are toxic for lymphocytes.<sup>10</sup> Therefore, it is considered that an ADA inhibitor may prevent adenosine released specifically at inflamed sites from metabolism by ecto-ADA and has great potential as an anti-inflammatory drug with few side effects.

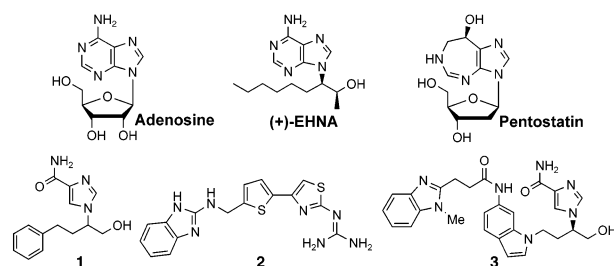


**Figure 1.** Chemical structures of adenosine and known ADA inhibitors.

A number of ADA inhibitors have been reported in the literature. However, almost all are purine nucleoside or alkyladenine analogues, for example, (+)-erythro-9-(2-hydroxy-3-nonyl)adenine ((+)-EHNA) (ground-state inhibitor),<sup>11</sup> pentostatin (transition-state inhibitor),<sup>12</sup> and various derivatives.<sup>13</sup> As a result, they have many problems, such as poor pharmacokinetics<sup>14</sup> and/or several toxicities.<sup>15</sup> Because of these problems, pentostatin is the only ADA inhibitor in clinical use; however, it is limited to the treatment of adult patients with hairy cell leukemia and is only available via intravenous administration.<sup>16</sup>

We considered that ADA inhibitors with reduced toxicity and oral bioavailability would be expected to not only improve the treatment of leukemia but also have potential use as anti-inflammatory drugs. We speculated that the problems of the known inhibitors could be improved by changing the nucleoside framework to a non-nucleoside framework. Despite the difficulty of converting a nucleoside to a non-nucleoside, a recent report from our laboratories described the discovery of a novel, highly potent non-nucleoside ADA inhibitor **3** ( $K_i = 7.7$  nM, human ADA) by intentional hybridization of the structurally distinct lead **1** ( $K_i = 5.9$   $\mu$ M) and **2** ( $K_i = 1.2$   $\mu$ M) by only two structure-based drug design (SBDD) iterations (Figure 1).<sup>17,18</sup> Further study of **3**, however, revealed its poor solubility and absorption (Table 1). On the other hand, in the first step of our hybridization process of **1** and **2**, **4** was designed (Figure 2). Compound **4** is still relatively weak in terms of ADA inhibitory activity ( $K_i = 680$  nM) but was considered as a good lead compound for optimization because of its simple, non-nucleoside framework and low molecular weight (MW), and moreover, the sum of hydrogen bond acceptors (Ha) and donors (Hd) is low compared to that of **3** (MW and Ha/Hd for **3** and **4** are 499.57 and 309.37, and 10/4 and 5/3, respectively) (Lipinski's rule<sup>19</sup>). Therefore, we attempted to optimize **4** based on a crystal structure of the **4**/ADA complex. In this paper, we disclose these optimization efforts and the discovery of a potent and orally bioavailable ADA inhibitor by a structure-based and metabolism-directed design approach.

Compound **4** was originally designed by introducing a hindered planar naphthyl ring in place of the phenyl ring of **1** in order to rotate the phenyl face of **1** and fit the narrow planar hydrophobic space (F1), which is occupied by the thiazole and thiophene rings of **2**.<sup>18</sup> The crystal structure of the **4**/ADA complex confirmed our

\* To whom correspondence should be addressed. Phone: +81-6-6390-1286. Fax: +81-6-6304-5435. E-mail: tadashi\_terasaka@po.fujisawa.co.jp.

<sup>†</sup> Medicinal Chemistry Research Laboratories.

<sup>‡</sup> Basic Research Laboratories.

<sup>§</sup> Current address: Department of Theoretical Drug Design, Graduate School of Pharmaceutical Sciences, Kyoto University, Sakyo-ku, Kyoto 606-8501, Japan.

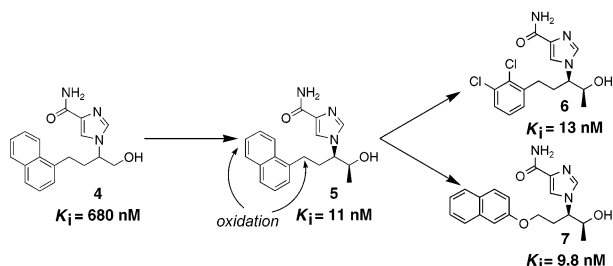
<sup>||</sup> Medicinal Biology Research Laboratories.

<sup>||</sup> Biopharmaceutical and Pharmacokinetic Research Laboratories.

**Table 1.** In Vitro Clearance with Liver Microsomes of Rat, Dog, and Human and Pharmacokinetic Parameters of **3** and **5–7** after po Administration to Rats and Dogs (10 mg/kg,  $n = 2–3$ )

	$K_i$ (nM) <sup>a</sup>	solubility ( $\mu\text{g/mL}$ ) <sup>b</sup>	in vitro clearance ( $\text{mL min}^{-1} \text{kg}^{-1}$ ) <sup>b</sup>			pharmacokinetic parameters in rats <sup>b</sup>			BA (%) <sup>c</sup>	
			rat	dog	human	$C_{\text{max}}$ ( $\mu\text{g/mL}$ )	$t_{1/2}$ (h)	AUC <sub>0–24h</sub> ( $\mu\text{g}\cdot\text{h/mL}$ )	rat	dog
<b>3</b>	7.7	4.2	35	97	123	<0.1	nd <sup>d</sup>	<0.1	nd <sup>d</sup>	nd <sup>d</sup>
<b>5</b>	11	481	307	30	45	1.25	0.66	1.37	30	38
<b>6</b>	13	500	111	21	4.5	1.63	1.66	2.11	44	43
<b>7</b>	9.8	80	79	11	3.8	0.97	1.12	1.85	42	91

<sup>a</sup>  $K_i$  values were measured with human ADA. Assays were performed in duplicate. <sup>b</sup> See Supporting Information. <sup>c</sup> BA = bioavailability. <sup>d</sup> nd = not determined.

**Figure 2.** Design process for discovery of **5–7**.

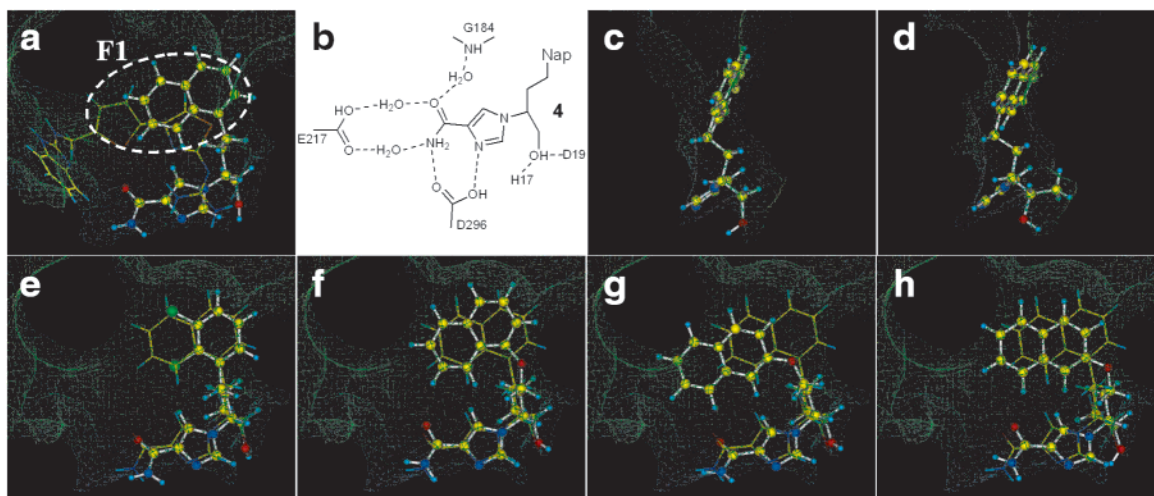
prediction (Figure 3a) and revealed that the imidazole-carboxamide group of **4** bound at the bottom of the catalytic site interacting with ADA through direct hydrogen bonds with Asp296 and via three water molecules and the hydroxyl group of **4** formed hydrogen bonds with His17 and Asp19 (Figure 3b). Furthermore, although **4** is racemic, only the (*R*)-stereoisomer was observed in the complex crystal as predicted by molecular modeling. Therefore, further studies were performed on the basis of the (*R*)-stereoisomer of **4**.

On the other hand, EHNA was designed by Schaeffer on the basis of studies on a large number of 9-substituted adenines 30 years ago<sup>20</sup> and further SAR studies about chirality and activity of various EHNA isomers have been reported to date.<sup>11</sup> Since the crystal structure of an EHNA/ADA complex has never been reported, the binding mode is not clear. However, a molecular modeling simulation suggested that the binding positions of the adenine and the hydroxyl group of EHNA were the same as those of the imidazolecarboxamide and the hydroxyl group of **4**, respectively. Moreover, (+)-EHNA has a (*S*)-methyl group at the  $\alpha$  position of the hydroxyl group. On the basis of the comparison described above, careful analysis of the interaction of **4** with the active site of ADA (Figure 3c) led to the prediction that a hydrophobic cavity exists and suggested introduction of a (*S*)-methyl group at the  $\alpha$  position of the hydroxyl group of **4**, the same as in EHNA. Therefore, to enhance the activity of **4**, we synthesized the compound with a (*S*)-methyl group at the  $\alpha$  position to the hydroxyl group, the (*2S,3R*)-isomer **5** (Figure 2). As a result, **5** showed high potency ( $K_i = 11$  nM) for ADA inhibition and was 60-fold more potent than **4**. This observation indicates that introducing a (*S*)-methyl group at the  $\alpha$  position to the hydroxyl group is effective to enhance activity. The crystal structure of the **5**/ADA complex verified that the (*S*)-methyl group was bound to the small hydrophobic cavity as predicted, and the other parts of **5** showed the same binding mode as **4** (Figure 3a–e).

Further metabolic study of **5** suggested formation of two principal metabolites that were monooxygenated derivatives of **5**. On the basis of its chemical structure, the two principal sites of metabolism of **5** could be

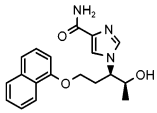
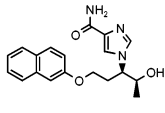
hypothesized (Figure 2): oxidation of the naphthyl ring and the benzylic position. Assuming that metabolism is the major route of clearance, chemical modification may lead to compounds with improved pharmacokinetics. In consideration of the narrow planar hydrophobic space available at F1 and protection of the designed compound from metabolism, a 2,3-dichlorophenyl ring was introduced in place of the naphthyl ring of **5**. The resulting **6** showed potent inhibitory activity ( $K_i = 13$  nM) similar to that of **5** (Figure 2). According to the binding mode of the **1**/ADA complex, **1** does not utilize the F1 space in binding, and moreover, the F1 space and the phenyl face of **1** are in a perpendicular relationship.<sup>18</sup> However, the crystal structure of the **6**/ADA complex confirmed that the 2,3-dichlorophenyl ring was indeed bound to the F1 space as predicted, and the other parts showed the same binding mode as **5** (Figure 3e). This observation suggests that replacement of the naphthyl ring of **5** with a 2,3-dichlorophenyl ring is effective in terms of ADA inhibitory potency.

On the other hand, according to the crystal structures of the **4**/ADA and **5**/ADA complexes, the naphthyl moiety is located at the entrance position of the enzyme and does not utilize the F1 space sufficiently (Figure 3a,e). That is, the hydrophobic space that is occupied by the thiophene ring of **2** is not utilized to bind these inhibitors. Therefore, we planned to use this space and block metabolism of the benzylic position in order to enhance activity and improve pharmacokinetics. Ether-linked analogues of **5**, which are substituted at the 1- or 2-position of the naphthyl ring, were considered (Table 2). Molecular modeling studies with ADA were performed to determine the best link position for the ether-linked compounds. Table 2 shows the simulated interaction and internal energies of the designed compounds. A 2-substituent was shown to be more stable than a 1-substituent because a 2-substituent has a higher interaction energy ( $\Delta E_{\text{interaction}} = 1.6$  kcal/mol) but much lower conformational strain energy ( $\Delta E_{\text{strain}} = -6.3$  kcal/mol) than a 1-substituent in order to fit to the active site. Certainly, it appeared from binding modes with ADA that the naphthyl moiety of a 1-substituted analogue is strained in order to fit to the active site without clashes with the enzyme wall, but the naphthyl ring of a 2-substituted compound utilizes the inner space of the active site in a good manner (Figure 3f,g). Therefore, we selected 2-substituted ether-linked **7** and only **7** was actually synthesized and evaluated. Consequently, **7** showed potent inhibitory activity similar to **5** (Figure 2). The crystal structure of the **7**/ADA complex revealed that although the 2-naphthoxy group shifted to the active-site entrance compared to the simulation, the other parts showed the same binding mode as **5** (Figure 3h).



**Figure 3.** Binding mode of inhibitors at the ADA active site. Accessible surfaces of the carbon atoms at the active sites are shown by the mesh. The upper portion of each figure is active site entrance (solvent region), and other nonmeshed black regions are occupied by protein: (a) binding orientations of **4** and **2** superimposed onto the active site surface of the **4**/ADA complex; (b) hydrogen bond networks around the carboxamide moieties of **4** (hydrogen bonds are shown by dashed lines); (c) view from the side by 90° of (a); (d) binding orientation of **5** (ball-and-stick)/ADA complex (PDB code, 1V78); (e) binding orientations of **6** and **5** superimposed onto the active site surface of the **5**/ADA complex; (f, g) simulated binding mode of ether-linked analogues of **5** to the active site of **5**/ADA complex; (h) binding orientations of **7** and **5** superimposed onto the active site surface of the **5**/ADA complex.

**Table 2.** Simulated Interaction Energies for Ether-Inserted Analogues of **5**

Structure		
$E_{\text{interaction}}$ (kcal/mol) <sup>a</sup>	-93.4	-91.8
$E_{\text{strain}}$ (kcal/mol) <sup>b</sup>	14.0	7.7

<sup>a</sup> Calculated interaction energies. <sup>b</sup> Differential of calculated internal energies.

Because the primary objective of this study was identification of ADA inhibitors with superior pharmacokinetics, **5–7** with potency similar to that of **3** were directly subjected to several pharmacokinetic experiments (Table 1). All three analogues displayed 20- to 120-fold better solubility than **3**, and upon oral dosing of **5** (10 mg/kg), a 1.25 μg/mL maximum plasma concentration ( $C_{\text{max}}$ ) and a 0.66 h plasma half-life ( $t_{1/2}$ ) were achieved (bioavailability BA = 30%), despite its high in vitro clearance in rat liver microsomes. In contrast, no detectable serum levels were observed with **3**. Compounds **6** and **7**, which were discovered by metabolism-directed design from **5**, displayed improved metabolic stability, since in vitro clearance was improved compared to **5**, especially, in dog and human liver microsomes. As anticipated from the metabolism study, **6** and **7** also exceeded **5** in most pharmacokinetic parameters, as shown in Table 1. Upon dosing rats with **6** (10 mg/kg), a substantial improvement of  $C_{\text{max}}$  (1.63 μg/mL), AUC (2.11 μg·h/mL), and  $t_{1/2}$  (1.66 h) were observed (BA = 44%). Dosing rats with **7** (10 mg/kg) led to a reasonable  $C_{\text{max}}$  (0.97 μg/mL) and some improvement of AUC (1.85 μg·h/mL) and better  $t_{1/2}$  (1.12 h) (BA = 42%). In particular, **7** displayed excellent oral bioavailability in dogs (BA = 91%).

Compounds **6** and **7** were next evaluated in in vivo models of inflammation and lymphoma. The in vivo antitumor activity of **6**, **7**, and pentostatin on lymphoma was evaluated in a SCID mouse model<sup>21</sup> (Table 3). Mice

**Table 3.** Comparative Antitumor Activity of **6** and **7** and Pentostatin on U937 Lymphoma Model

drug	dose (mg/kg) <sup>b</sup>	MST (day)
control		22.0
AraA		23.5
<b>6</b> <sup>a</sup> (po)	10 (b.i.d.)	34.0
	32 (b.i.d.)	42.5
	32 (u.i.d.)	38.0
<b>7</b> (po)	10 (b.i.d.)	30.0
	32 (b.i.d.)	35.5
	32 (u.i.d.)	30.0
pentostatin (ip)	0.025	28.5
	0.25	34.0
	2.5	42.5

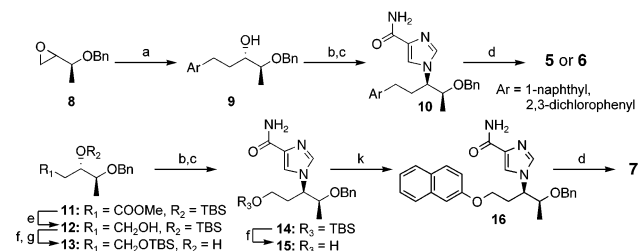
<sup>a</sup> HCl salt. <sup>b</sup> b.i.d. = twice daily dosing. u.i.d. = once daily dosing.

inoculated with U937 cells were unhealthy in appearance and had swollen abdomens. The median survival time (MST) was 22.0 days. Oral administration (po) of **6** at 32 mg/kg u.i.d. and b.i.d. with the antitumor 9-β-D-arabinofuranosyladenine (AraA) resulted in improved survival with MST of 38.0 and 42.5 days, respectively. Mice treated with **7** at 10 and 32 mg/kg survived significantly longer (MST of 30–35.5 days) than control mice. Pentostatin prolonged the life of mice bearing U937 in a dose-dependent manner. The MST of pentostatin (2.5 mg/kg) with AraA was 42.5 days. Compound **6** had antitumor activity against lymphoma in combination with AraA because it prolonged the survival time of SCID mice inoculated with U937 cells and exhibited oral activity comparable to that observed for intraperitoneal administration (ip) of pentostatin.

Furthermore, in the adjuvant arthritis model in rats, **6** also showed an anti-inflammatory effect orally (ED<sub>30</sub> = 1.6 mg/kg po). This is the first report of in vivo anti-inflammatory efficacy for an ADA inhibitor after oral administration.

The syntheses of **5–7** are outlined in Scheme 1. The reaction of epoxide **8**<sup>22</sup> with the suitable aryl Grignard reagent, prepared in situ, and separation of the dia-



Scheme 1<sup>a</sup>

<sup>a</sup> Reagents and conditions: (a) ArCH<sub>2</sub>Cl, Mg, LiCl, CuCl<sub>2</sub>, Et<sub>2</sub>O, -78 °C to room temp, overnight; (b) MsCl, Et<sub>3</sub>N, CH<sub>2</sub>Cl<sub>2</sub>, 0 °C, 1 h; (c) 4-imidazolecarboxamide, NaH, DMF, 70 °C, 24 h; (d) Pd(OH)<sub>2</sub>, cyclohexene, EtOH, 90 °C, 30 min or TMSI, CHCl<sub>3</sub>, 0 °C to room temp, overnight; (e) LiAlH<sub>4</sub>, Et<sub>2</sub>O, 0 °C, 30 min; (f) TBAF, THF, 0 °C, 1 h; (g) TBSCl, imidazole, DMF, 0 °C to room temp, overnight; (h) (1) MsCl, Et<sub>3</sub>N, CH<sub>2</sub>Cl<sub>2</sub>, 0 °C; (2) K<sub>2</sub>CO<sub>3</sub>, DMF, 60–70 °C, 6 h.

stereoisomers gave alcohol **9**. The secondary alcohol moiety of **9** was then converted to mesylate, and displacement by S<sub>N</sub>2 reaction with 4-imidazolecarboxamide in the presence of NaH in DMF afforded **10**. Compounds **5** and **6** were obtained by debenzoylation of the corresponding **10**.

The reduction of the ester group of **11**<sup>23</sup> with LiAlH<sub>4</sub> in Et<sub>2</sub>O at 0 °C gave the primary alcohol **12**. Removal of the *tert*-butyldimethylsilyl (TBS) group with tetrabutylammonium fluoride (TBAF) followed by selective protection of the primary alcohol afforded the TBS protected secondary alcohol **13**. Compound **14** was prepared by procedures similar to those for **10**. After removal of the TBS group of **14**, the resulting alcohol **15** was converted to mesylate, followed by displacement with the 2-naphthoxy group in the presence of K<sub>2</sub>CO<sub>3</sub> in DMF to afford **16**. Deprotection of the benzyl group afforded **7**.

In summary, we report optimization efforts based on **4**, and the discovery of potent and orally bioavailable ADA inhibitors by a structure-based and metabolism-directed design approach. As a result, we achieved not only a drastic improvement in activity compared to that of **4** but also a drastic improvement in oral bioavailability compared to that of **3**. Furthermore, **6**, discovered in this study, demonstrated *in vivo* efficacy in models of inflammation and lymphoma. This is the first report of *in vivo* efficacy for an ADA inhibitor after oral administration.

**Acknowledgment.** The authors are grateful to The Chemo-Sero-Therapeutic Research Institute for the gift of pentostatin. We thank Hiroyoshi Sakai for metabolism studies and Dr. David Barrett for valuable comments and help in the preparation of the manuscript.

**Supporting Information Available:** Experimental details and analytical data of compound synthesis and assay. This material is available free of charge via the Internet at <http://pubs.acs.org>.

## References

- Cristalli, G.; Costanzi, S.; Lambertucci, C.; Lupidi, G.; Vittori, S.; Volpini, R.; Camaioni, E. Adenosine deaminase: Functional implications and different classes of inhibitors. *Med. Res. Rev.* **2001**, *21*, 105–128.
- Resta, R.; Thompson, L. F. SCID: the role of adenosine deaminase deficiency. *Immunol. Today* **1997**, *18*, 371–374.
- Valenzuela, A.; Blanco, J.; Callebaut, C.; Jacotot, E.; Lluís, C.; Hovanessian, A. G.; Franco, R. Adenosine deaminase binding to human CD26 is inhibited by HIV-1 envelope glycoprotein gp120 and viral particles. *J. Immunol.* **1997**, *158*, 3721–3729.

- (a) Nakamachi, Y.; Koshiba, M.; Nakazawa, T.; Hatachi, S.; Saura, R.; Kurosaka, M.; Kusaka, H.; Kumagai, S. Specific increase in enzymatic activity of adenosine deaminase 1 in rheumatoid synovial fibroblasts. *Arthritis Rheum.* **2003**, *48*, 668–674. (b) Yüksel, H.; Akoglu, T. F. J. Serum and synovial fluid adenosine deaminase activity in patients with rheumatoid arthritis, osteoarthritis, and reactive arthritis. *Ann. Rheum. Dis.* **1988**, *47*, 492–495.
- (a) Smith, J. F.; Poplack, D. G.; Holiman, B. J.; Leventhal, B. G.; Yarbro, G. Correlation of adenosine deaminase activity with cell surface markers in acute lymphoblastic leukemia. *J. Clin. Invest.* **1978**, *62*, 710–712. (b) Simpkins, H.; Stantai, A.; Davis, B. H. Adenosine deaminase activity in lymphoid subpopulations and leukemias. *Cancer Res.* **1981**, *41*, 3107–3110.
- Cronstein, B. N. Adenosine, An endogenous antiinflammatory agent. *J. Appl. Physiol.* **1994**, *76*, 5–13.
- Ohta, A.; Sitkovsky, M. Role of G-protein-coupled adenosine receptors in downregulation of inflammation and protection from tissue damage. *Nature* **2001**, *414*, 916–920.
- (a) Rudolph, K. A.; Schubert, P.; Parkinson, F. E.; Fredholm, B. B. Neuroprotective role of adenosine in cerebral ischemia. *Trends Pharmacol. Sci.* **1992**, *13*, 439–445. (b) Marquardt, D. L.; Gruber, H. E.; Wasserman, S. I. Adenosine release from stimulated mast-cells. *Proc. Natl. Acad. Sci. U.S.A.* **1984**, *81*, 6192–6196.
- Kameoka, J.; Tanaka, T.; Nojima, Y.; Schlossman, S. F.; Morimoto, C. Direct association of adenosine deaminase with T cell activation antigen, CD26. *Science* **1993**, *261*, 466–469.
- Franco, R.; Valenzuela, A.; Lluís, C.; Blanco, J. Enzymatic and extraenzymatic role of ecto-adenosine deaminase in lymphocytes. *Immunol. Rev.* **1998**, *161*, 27–42.
- Baker, D. C.; Hanvey, J. C.; Hawkins, L. D.; Murphy, J. Identification of the bioactive enantiomer of erythro-3-(adenine-9-yl)-2-nonanol (EHNA), a semi-tight binding inhibitor of adenosine deaminase. *Biochem. Pharmacol.* **1981**, *30*, 1159–1160.
- Agerwal, R. P.; Spector, T.; Parks, R. E. Tight-binding inhibitors IV. Inhibition of adenosine deaminase by various inhibitors. *Biochem. Pharmacol.* **1977**, *26*, 359–367.
- Cristalli, G.; Costanzi, S.; Lambertucci, C.; Lupidi, G.; Vittori, S.; Volpini, R.; Camaioni, E. Adenosine deaminase: Functional implications and different classes of inhibitors. *Med. Res. Rev.* **2001**, *21*, 105–128 and references therein.
- (a) McConnell, W. R.; Furner, R. L.; Hill, D. L. Pharmacokinetics of 2'-deoxycofornycin in normal and L1210 leukemic mice. *Drug Metab. Dispos.* **1979**, *7*, 11–13. (b) McConnell, W. R.; El-Dareer, S. M.; Hill, D. L. Metabolism and disposition of erythro-9-(2-hydroxy-3-nonyl)[<sup>14</sup>C] adenine in the rhesus monkey. *Drug Metab. Dispos.* **1980**, *8*, 5–7.
- Brogden, R. N.; Sorokin, E. M. Pentostatin. A review of its pharmacodynamic and pharmacokinetic properties, and therapeutic potential in lymphoproliferative disorders. *Drugs* **1993**, *46*, 652–677.
- Rafel, M.; Cervantes, F.; Beltran, J. M.; Zuazu, J.; Nieto, L. H.; Rayon, C.; Talavera, J. G.; Montserrat, E. Deoxycofornycin in the treatment of patients with hairy cell leukemia. *Cancer* **2000**, *88*, 352–357.
- Terasaka, T.; Nakanishi, I.; Nakamura, K.; Eikyu, Y.; Kinoshita, T.; Nishio, N.; Sato, A.; Kuno, M.; Seki, N.; Sakane, K. Structure-based de novo design of non-nucleoside adenosine deaminase inhibitors. *Bioorg. Med. Chem. Lett.* **2003**, *13*, 1115–1118.
- Terasaka, T.; Kinoshita, T.; Kuno, M.; Nakanishi, I. A highly potent non-nucleoside adenosine deaminase inhibitor: Efficient drug discovery by intentional lead hybridization. *J. Am. Chem. Soc.* **2004**, *126*, 34–35.
- Lipinski, C. A.; Lombardo, F.; Dominy, B. W.; Feeney, P. J. Experimental and computational approaches to estimate solubility and permeability in drug discovery and development settings. *Adv. Drug Delivery Rev.* **1997**, *23*, 3–25.
- Schaeffer, H. J.; Schwender, C. F. Enzyme Inhibitors. 26. Bridging hydrophobic and hydrophilic regions on adenosine deaminase with some 9-(2-hydroxy-3-alkyl)adenines. *J. Med. Chem.* **1974**, *17*, 6–8.
- Niitsu, N.; Yamamoto-Yamaguchi, Y.; Kasukabe, T.; Okabe-Kado, J.; Umeda, M.; Honma, Y. Antileukemic efficacy of 2'-deoxycofornycin in monocytic leukemia cells. *Blood* **2000**, *96*, 1512–1516.
- Terasaka, T.; Nakamura, K.; Seki, N.; Kuno, M.; Tsujimoto, S.; Sato, A.; Nakanishi, I.; Kinoshita, T.; Nishio, N.; Okumura, H.; Tsuji, K. WO 00/05217, 2000.
- Reetz, M. T.; Raguse, B.; Marth, C. F.; Hugel, H. M. A rapid injection NMR study of the chelation controlled Mukaiyama aldol addition: TiCl<sub>4</sub> versus TiCl<sub>4</sub> as the Lewis acid. *Tetrahedron* **1992**, *48*, 5731–5742.